AAPS PharmSciTech (© 2010)
DOI: 10.1208/s12249-010-9542-5

Research Article

Micronization of a Soft Material: Air-Jet and Micro-Ball Milling

Imran Y. Saleem[1,3] and Hugh D. C. Smyth[2]

Received 2 February 2010; accepted 8 November 2010

Abstract. The air-jet and ball-mill are frequently used in fine micronization of active pharmaceutical ingredients to the order of 1–5 μm, which is important for increasing dissolution rates, and also for pulmonary delivery. In this study, we investigated the ability of air-jet and ball-mill to achieve adequate micronization on the lab scale using a model soft material, Pluronic® F-68. Material mechanical properties were characterized using the nanometer 600. Pluronic® F-68 was ball-milled in a micro-mill at different material weights and durations in liquid nitrogen vapor. In comparison, a lab scale air-jet mill was used at various milling parameters according to a full factorial design, where the response factors were particle yield and particle size distribution, which was analyzed using laser diffraction and scanning electron microscopy. The yield achieved with the micro-ball mill was 100% but was ~80% for the air-jet mill, which reduced the size of Pluronic® F-68 from 70 μm to sizes ranging between 23–39 μm median diameters. Ball milling produced particles less than 10 μm after 15 min. Although air-jet milling proved capable of particle size reduction of the relatively soft material Pluronic® F-68, limitations to the lower size range achievable were observed. The feed rate of the material into the air jet mill was a significant factor and slower feed rates lead to smaller sizes by allowing more time for particle collisions and subsequent particle breakage to occur. Micro-ball milling under cold condition was more successful at achieving a lower range particle size reduction of soft materials.

KEY WORDS: aerosolisation; air-jet mill; cryo-micro-ball mill; micronization; soft material.

INTRODUCTION

Micronization of materials is a common process in many aspects of pharmaceutical manufacturing. Although much is known on the particle size reduction of hard and crystalline materials, few studies have investigated the milling of softer materials. In addition, many drugs in the pharmaceutical industry are of low aqueous solubility and thus dissolution rate becomes a limiting factor for bioavailability. It is well known that one approach to this problem is to perform particle size reduction, resulting in very fine particles and a larger surface area leading to an increase dissolution rate and consequently, bioavailability (1,2). In addition, a fine particle size is required for drugs administered via the pulmonary route (3,4). Pulmonary delivery of drugs via dry powder inhalers (DPIs) have the advantage of eliminating solubility and stability concerns common with other aerosol generation methods (5,6). However, the airways remain a very efficient barrier to delivery with particles larger than 5 μm deposited in the mouth and esophagus (7). Generally, particles 5 μm (aerodynamic diameter) or less are deposited in the bronchioles and those 1 μm or less reaching the alveoli (8). As a result, micronization of particles has become important in pulmonary drug delivery to achieve the desired targeted deposition of the therapeutic agent (9,10). Of emerging importance in these areas are drugs and excipients with different physical properties to traditional crystalline low molecular weight substances. In these studies, our focus was to determine the performance and efficiency of two typical milling methods when soft particles were to be micronized.

There are several types of mills available for particle size reduction; but, currently, only the air-jet fluid energy mill and ball-mill are commonly used to reduce the particle size to 5 μm or less in dry conditions (11). Furthermore, both are available on a small bench top scale, ideal for laboratory use, and have the advantages of high milling efficiency, ability to mill compounds of different hardness and strength, and can be used with low batch sizes (11). In an air-jet mill, the material passes into the grinding chamber via a vibrating feeder which controls the feed rate. Particles are accelerated to a high velocity by air jets passing through a "pusher" nozzle prior to entering the grinding chamber, where the material undergoes extreme turbulence due to high pressure and velocities generated from air flow introduced via the two "grinding" nozzles. The turbulence and orbital nature of the grinding chamber ensures multiple particle–particle and particle–wall interactions occur at a high frequency and induces particle fracture and size reduction. A ball mill is also commonly employed for fine grinding. In a ball mill, grinding energy is transferred to materials through media such as balls,

[1] School of Pharmacy and Biomolecular Sciences, Liverpool John Moores University, Liverpool, L3 3AF, UK.
[2] College of Pharmacy, University of Texas at Austin, Austin, Texas 78712, USA.
[3] To whom correspondence should be addressed. (e-mail: I.Saleem@ljmu.ac.uk)

1530-9932/10/0000-0001/0

rods, pebbles, by moving the mill body (12). For both types of mills the mechanisms by which particle size is reduced follow the same principles. The kinetics of this process may be derived by applying the stochastic theories derived by Gilvarry (13), Gaudin and Meloy (14), or Callcot (15). These theories are based on the idea that cracks on the micro- or nanoscale are present in the particles, and these are activated when the particle experiences stress and absorb elastic strain energy. The cracks develop rapidly and collide with each other to cause particle fracture. Similarly, the dynamics of particle micronization has also been described previously by Chujo (16).

Powder behaviors during micronization are influenced by mechanical properties such as hardness and elasticity of the material (Young's modulus; 11). The hardness of a material determines its resistance to plastic deformation and can be calculated from load–displacement graphs obtained during indentation experiments (expressed as the ratio of applied force to the area of indentation; 17). The elasticity determines the resistance of the material to elastic deformation and can be obtained from the slope of the unloading curve on the load–displacement graph. For particle size reduction to occur, permanent deformation of the material must occur. Thus, the energy provided for particle interactions must overcome the elastic properties of the material. This would allow for fracture to occur leading ultimately to size reduction and permanent deformation.

In combination with assessing micronization performance in these studies, it was essential to obtain an understanding of the mechanical properties of the model soft powder particles. The development of new indentation techniques has led to improved mechanical characterization of powders. Generally, this is determined from the loading and unloading of an indenter into the sample surface from which the mechanical properties, including hardness and elasticity, of the material can be analyzed. Hardness of powders has been determined using microindentation on compaction of powders. However, the disadvantages with this method include the requirements of large sample weights, changes in mechanical properties during compaction (17), as well as porosity (18) and particle size (19). Consequently, nanoindentation enables the measurements of mechanical properties of powders using very small sample quantities without the need for compaction.

We are unaware of any literature describing the use of air jet mills and ball mills for soft materials. Only one study has investigated the optimization conditions for hard materials (lactose and sucrose) in a lab scale air-jet mill (11). In this study, we used a model soft material, Pluronic® (Poloxamer), which are alkylene copolymers consisting of ethylene oxide and propylene oxide and have broad pharmaceutical applications (20–22). Pluronic® F-68 was chosen as a model drug to investigate the optimum operating conditions to achieve particle sizes suitable for pulmonary drug delivery, due to its characterized physicochemical properties and the material's mechanical properties, which offer a contrast to the more traditional hard crystalline materials generally used. Moreover, Pluronic® F-68 has wide pharmaceutical applications that could enable it to be used as an excipient (23) or even an active material (24) in DPIs. Additionally, we investigated optimal milling conditions for Pluronic® F-68 using a full factorial experimental design that investigates the effects of powder feed rates, "pusher" nozzle pressures and "grinding" nozzle pressures to achieve particle size reduction in an air-jet mill suitable for DPIs. Furthermore, due to the physicochemical properties of Pluronic® F-68 and from preliminary experiments, plastic deformation of Pluronic® F-68 was observed using the micro-ball mill. Hence, liquid nitrogen was used to chill the milling chamber, prevent plastic deformation, and enhance the particle fracture process. Incorporation of liquid nitrogen (cryo-milling) is a common technique used for micronization of materials by a number of investigators (23,25–27). Hence, comparisons were made between cryo-micro-ball milling and air-jet milling to achieve optimum conditions for micronization of Pluronic® F-68.

MATERIALS AND METHODS

Materials

Pluronic® F-68 was purchased from BASF (Shreveport, LA, USA)

Methods

Physical Characterization of Pluronic® F-68

Particle Size Analysis and Morphology. The particle size (Dv50 and Dv90) of unmilled Pluronic® F-68 was determined using collected fractions from sieving (125, 107.5, 82.5, 69, 54, 38.5, 26, and 10 μm) and plotting a cumulative oversize distribution curve. Particle size characteristics of Pluronic® F-68 after milling were determined using a Sympatec Helos laser diffraction instrument (Sympatec GmbH, Germany) equipped with a R3 lens. Three measurements of particle size were performed for each experimental milling condition (n=3). Briefly, Pluronic® F-68 was dispersed using compressed nitrogen gas at 150 psi. The aerosol was drawn through the laser sensing region using a relative pressure of 95 mbar, and the detector was activated at a minimum optical concentration of between 4% and 5%. Morphology and particle size were further analyzed using scanning electron microscopy (SEM) (JEOL 5800LV Scanning Electron Microscope) in low pressure mode.

Hardness/Elasticity Determination for Pluronic® F-68. Particles of Pluronic® F-68 were held in place on a microscope slide containing a drop of non-viscous adhesive (3D-Creation Enterprise Co Ltd). The microscope slide was then attached to a Nanotester sample holder using the same adhesive, and nanoindentation was performed using a Nanotester 600 (Micro Materials, Wrexham, UK). This instrument contained a diamond three-sided pyramid indenter attached to a pendulum, which was loaded against the powder by passing a current through a coil drawing it towards a magnet. The depth the indenter entered into the surface of the powder depended upon the variation in voltage between the capacitance plates. The sample holder was aligned with the indenter on a stage incorporating a high-resolution microscope, which made it possible for high-precision indentation of selected areas. Nanoindentations were

performed at 40 mN using a loading rate of 0.37 mN s^{-1}. Hardness was analyzed from the load–displacement curves generated using the computer software provided.

Air-Jet Micronization

Micronization of Pluronic® F-68 using Air-Jet Fluid Energy Mill. Pluronic® F-68 (1 g) was fed into the air-jet mill (Aljet mill, Fluid Energy, Plumsteadville, PA, USA) using a vibratory feeder and sample was collected and analyzed from the collecting chamber only. The particle size and morphology before and after milling was evaluated using laser diffraction and SEM as described above.

The milling of Pluronic® F-68 was investigated using a full factorial design incorporating two feed rates and varying both "grinding" ("1" and "2") and "pusher" nozzles between 50 and 100 psi (Table 1), with each experiment performed in triplicate. The response factors for the experimental design analysis were particle size distribution (Dv50, Dv90) and yield (%). The Dv50 and Dv90 represent the 50^{th} and the 90^{th} percentile, respectively, of the particle size distribution.

Air-Jet Micronization Incorporating the Next Generation Impactor. Optimized air-jet milling conditions obtained from the design of experiment described above were used in a modified air-jet mill set up. In these experiments, the outlet of the air-jet mill was fed directly into a next-generation impactor (NGI) (MSP Corp, Minneapolis, MN), from which, pre-classified and acceptable (for inhalation) materials could be captured and the yield calculated. Briefly, the air-jet mill was connected to the inlet of the NGI and 1 g Pluronic® F-68 was fed through the air-jet mill using a vibratory feeder. A vacuum at 60 L/min was used to draw the Pluronic® F-68 through the air-jet grinding chamber into the NGI, with 5 ml water added to stage 1 of the NGI to prevent large particles from passing into the smaller stages via reintrainment. The particles were collected from stage 3 and analyzed using laser diffraction (Dv50) and SEM as above.

Micronization of Pluronic® F-68 using Cryo-Micro-Ball Mill. Pluronic® F-68 of different weights (25, 50, and 100 mg) were placed into a micro-ball mill vessel (Dentsply Rinn Corporation, Elgin, IL, USA) containing a single stainless steel ball bearing of diameter ~0.5 cm. The micro-ball mill, containing the powder was immersed in liquid nitrogen for 30 s and milled at various times (5, 10, and 15 min) for each weight of Pluronic® F-68 by placing the chamber in liquid nitrogen vapor. Experiments were repeated in triplicates. The micro-ball mill was attached to a cordless Skil HD4570 Jig Saw (Bosch Tool Corp, Mount Prospect, IL, USA, Model No. F012457000) and the speed setting used was 'FAST'. Particle size and morphology was analyzed using laser diffraction and SEM as above

Table I. Full Factorial Design of Micronizing Pluronic® F-68 Using the Aljet Mill

Feed rate (g/min)	Grinding nozzle '1' (psi)	Grinding nozzle '2' (psi)	Pusher nozzle (psi)
0.14 or 1	60 or 100	60 or 100	50 or 100

Statistical Analysis

For experiments regarding the air-jet mill, the statistical analysis was performed using Design Expert 5 (Stat-Ease Corp, Minneapolis, MN) software for designing and analyzing factorial experiment designs. The data was analyzed by this software using ANOVA and post-hoc comparisons tests. Differences of $p<0.001$ were considered significantly different.

All statistical analysis for experiments via the cryo-micro-ball mill was performed using the paired Student's *t*-test with two-tailed comparison. Differences of $p<0.05$ were considered significantly different.

RESULTS

Hardness of Pluronic® F-68

Figure 1 represents a typical load–displacement curve of Pluronic® F-68 obtained from using the Nanotester 600. The loading phase rises with an upward concave curvature, followed by a holding portion of the indentation, during which the force remains constant and the indenter continues to penetrate into the particle, defined as the strain rate at constant stress. Finally, the slope of the unloading curve was concave in shape, with the initial portion of the slope very small indicating high elastic coil. The initial region of the unloading slope was related to the stiffness, which was the change in force with a change in penetration depth and can be related to elasticity. Hardness of the material was determined as the resistance to deformation when the indenter was pressed into the surface and was calculated as the applied load divided by the projected area of contact. The maximum applied load was 10.07 mN providing a hardness value of 0.05 GPa with a Young's modulus of 0.76 GPa. The hardness value was at least 10-fold less than the value obtained for a more crystalline material, such as sucrose (0.64 GPa), while the Young's modulus was almost a 100-fold less (32 GPa) (28,29).

Air-Jet Fluid Energy Mill

For clarity, only the factors which proved to be statistically significant are represented below. To explain the relationship between feed rate, grinding '1', grinding '2' nozzles, and pusher pressure nozzle on Dv50, Dv90, and Yield, a least-squares regression was performed on the factorial design data. Based on these equations, interactions, and significant factors were plotted on cube and contour plots to determine the optimal conditions within the design space.

Particle Size

The Dv50 and Dv90 of the unmilled Pluronic® F-68 was 70 and 86 μm, respectively. During the milling process the Dv50 was most significantly ($p<0.001$) influenced by the combination of feed rate and grinding pressure '1', which had an inversely proportional relationship irrespective of pusher or grinding '2' pressures (Fig. 2a, b). The results also indicated that a high pusher pressure and low grinding '2' helped achieve the smallest particle size (Fig. 2a).

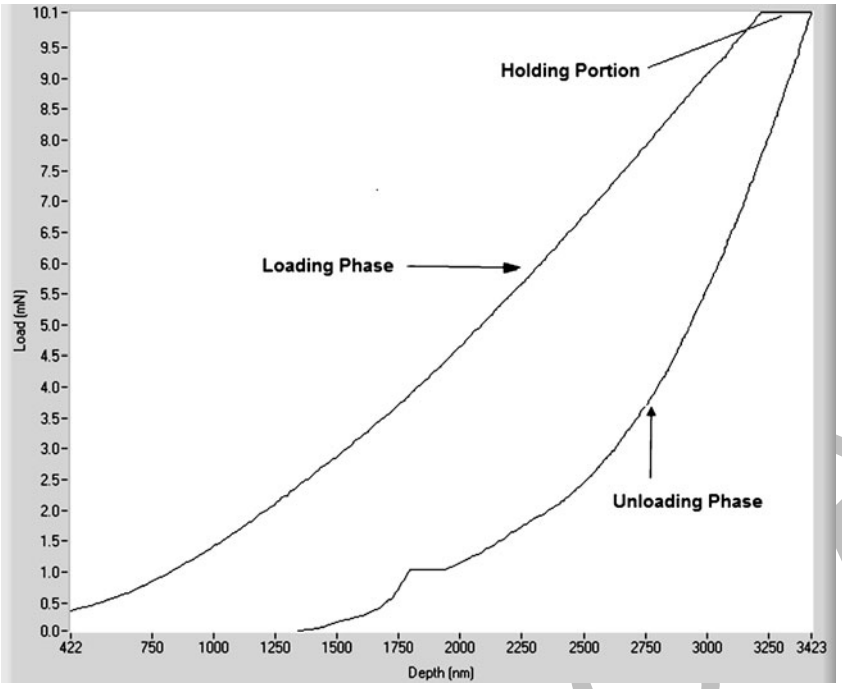

Fig. 1. Load–displacement profile of Pluronic® F-68 using the Nanotester 600

The most significant factor influencing the Dv90 particle size distribution was feed rate. When combined with grinding pressure '1' nozzle, an inversely proportional relationship was seen (Fig. 2c, d) (i.e., an increase in grinding '1' resulted in a decrease in Dv90). The results also confirmed that a high pusher pressure and low grinding '2' helped achieve the smallest particle size (Fig. 2c).

However, particle size reduction was quite modest in these experiments. The inability of the air-jet mill to reduce the Dv50 particle size to less than 24 μm was also confirmed by SEM (Fig. 3). The bulk Pluronic® F-68 (Fig. 3a) had a spherical appearance and size of approximately 50 μm. When the Pluronic® F-68 was air-jet milled, the particle size observed by SEM corresponded with that obtained using laser diffraction (25 μm) (Fig. 3b). As expected, the milling process changed the morphology of the particles and there was a broader distribution of size ranges within the sample. Notably, the particles did undergo significant particle size reduction under all of the air-jet milling parameters used.

Inertial Classification

Using optimized milling conditions derived from studies described above, milled particles were separated by inertial impaction, so that powders with smaller sizes and narrow size distributions could be collected and analyzed.

Particle Size and Yield

The samples were collected from stage 3 of the NGI (cut-off diameter 4.6 μm). The particle size results (Table 2) indicated that milling into NGI achieved Dv50 particle size close to 5 μm, however with a low yield, 1.9% achieved from 1 g Pluronic® F-68 starting material, indicating the poor efficiency of this method, compared with over 80% yield achieved from the air-jet mill.

Cryo-Micro-Ball Mill

The main parameter influencing particle size of Pluronic® F-68 powder using cryo-micro-ball method was milling duration (Table 3). As milling time increased from 5 to 15 min there was a significant decrease in particle size using milling masses of 25 and 100 mg loaded into the micro-ball mill ($p < 0.05$).

After 15 min, all Pluronic® F-68 samples, regardless of mass, were reduced in particle size to less than 10 μm, which was significantly less than using the optimized parameters of the air-jet mill (Dv50=24.79 μm). Comparing the SEMs to the bulk and air-jet milled Pluronic® F-68 (Fig. 3); the cryo-micro-ball milled Pluronic® F-68 samples lost their spherical structure and shape, and became more flat in appearance (Fig. 4).

DISCUSSION

Physical Characteristics

The extent of particle size reduction is dependent on the elastic–plastic properties of the material which determine the resistance to breaking and the propagation of fracture (29). Thus, parameters such as hardness and Young's modulus have an important role in size reduction. It is generally accepted that hard and elastic materials require much higher energies than soft and inelastic materials for particle breakage to occur (29). This is due to more energy required to overcome the elastic properties of the material, resulting in deformation and fracture, eventually leading to particle break

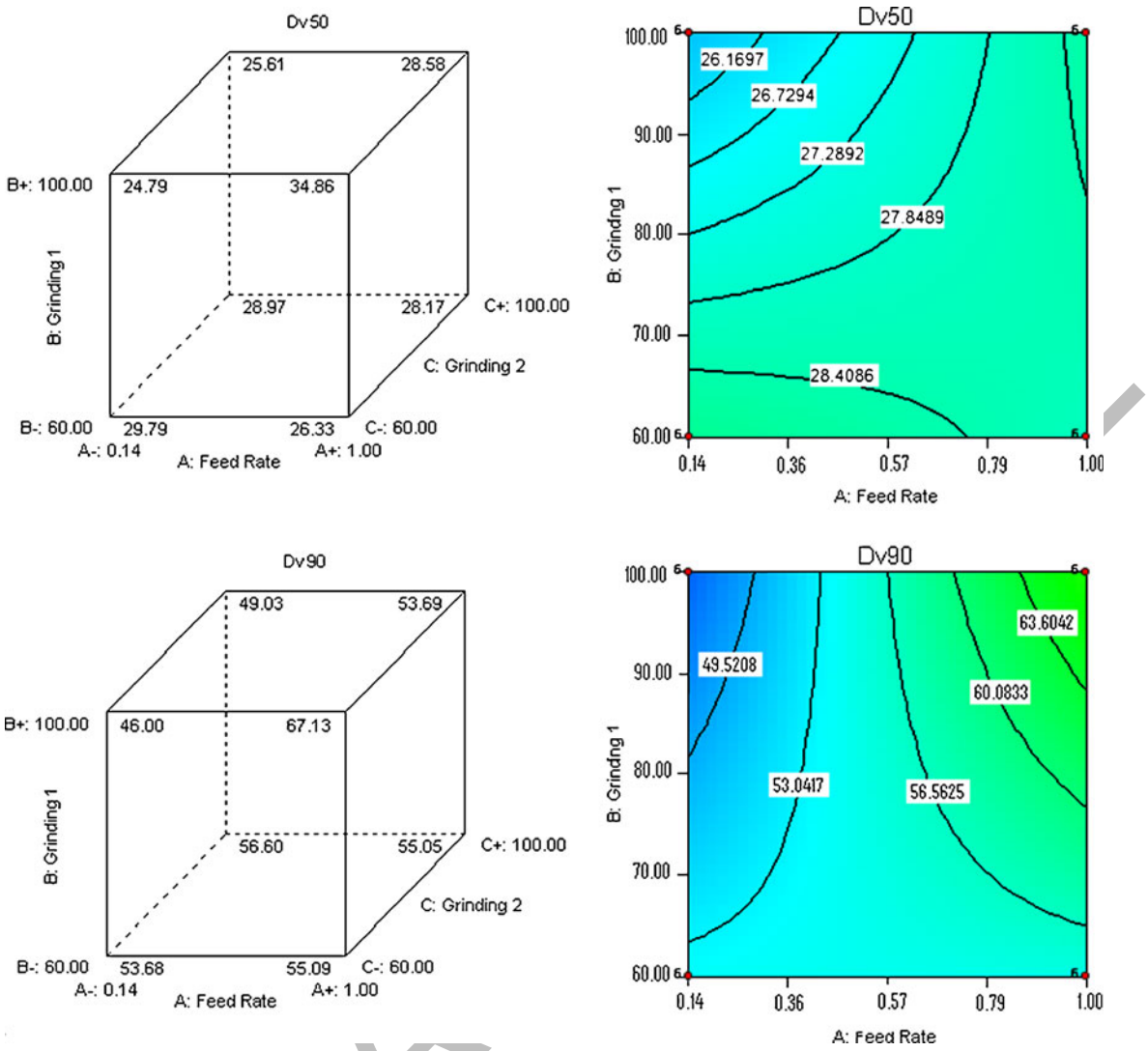

Fig. 2. Dv50 (**a** cube, **b** contour plot) and Dv90 (**c** cube, **d** contour plot) values of micronized Pluronic® F-68 at different feed rate, grinding '1', grinding '2', and at high pusher pressure (100 psi)

up. The loading displacement curves (Fig. 1) do not overlap, but show the typical hysteresis indicating both elastic and plastic behavior associated with the soft material, Pluronic® F-68. The small force penetrating the Pluronic® F-68, applied from the indenter, and large displacement during loading of approximately 3000 nm indicated a very soft surface (Fig. 1). The hardness value was 10-fold less, while the Young's modulus was almost 100-fold less than the hard sucrose

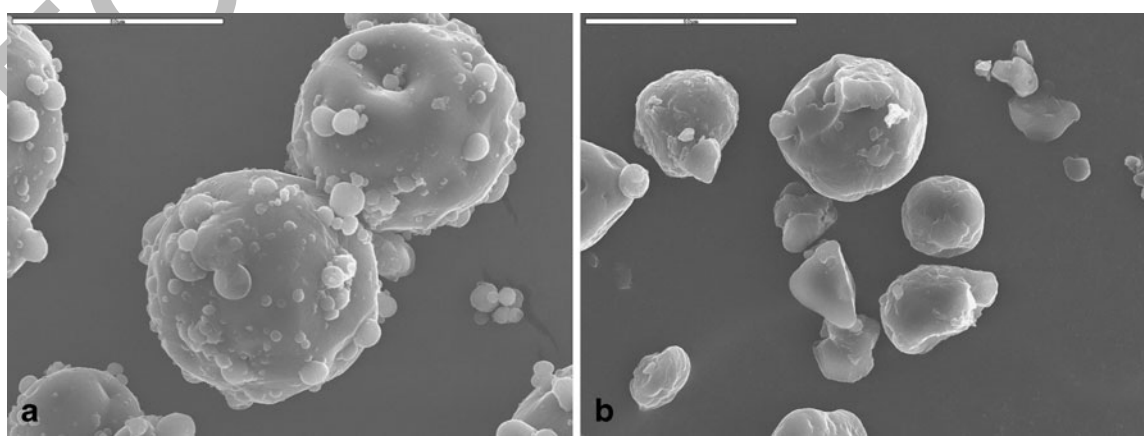

Fig. 3. SEM micrographs of bulk Pluronic® F-68 (**a**) and air jet milled (**b**) The scale bar is 50 μm

Table II. Particle Size of Pluronic® F-68 Milled into NGI and Collected at Stage 3 (n=3).

NGI Stage	Dv50 (μm)	Yield (%)
3	5.59±1.19	1.9

(0.64 GPa, 32 GPa; 28) and soft elastic sodium stearate (0.65 GPa, 37 GPa) (30) or sodium chloride (0.44 GPa, 46.5 GPa) materials, respectively (29).

The differences in particle size reduction of Pluronic® F-68 compared with the hard crystalline sucrose can be explained in terms of hardness and elasticity. Studies optimizing particle size reduction of sucrose using an air-jet mill reported median particle sizes as small as 2.92 μm (Dv50) and 8.58 μm (Dv90) using a feed rate of 1.8 g/min, pusher pressure at 110 psi and grinding pressure at 65 psi (11). However, in this study similar optimum milling conditions as performed by vatsaraj *et al.* (11), resulted in more coarse products and a larger particle size distribution (Dv50: 26.33 μm, Dv9: 55.09 μm). Pluronic® F-68 is a much softer material than sucrose, and thus it was expected to have a smaller size at the same milling condition parameters. However, Pluronic® F-68 has high elastic properties (Fig. 1) as indicated by the small initial slope on the unloading curve. Therefore higher pressures (grinding '1', '2', and pusher nozzles) were required to induce particle fracture and breakage. Consequently, the smallest particle size obtained by air-jet milling was 24 μm (Dv50) and 46.0 μm (Dv90) [low feed rate (0.14 g/min), grinding '1' (100 psi), grinding '2' (60 psi), pusher pressure (100 psi)], an order of magnitude 10-fold higher than the smallest particle size achieved with sucrose.

Air-Jet Fluid Energy Mill

Effect of Feed Rate, Pusher and Grinding Nozzle Pressures on Particle Size Reduction and Yield in an Air-Jet Mill

A lower feed rate was imperative at reducing particle size and may allow more energy input to fewer particles over time resulting in more efficient particle–particle interactions to occur within the grinding chamber resulting in particle deformation and fracture, and eventually leading to size reduction. It is proposed that when the feed rate was increased, the energy input from the pusher and grinder nozzles was distributed over a larger number of particles reducing the kinetic energies of each. Consequently, this may have corresponded to less high-speed particle–particle collisions within the milling chamber. Therefore, at the pressures used within this study, a feed rate of 1 g/min was too fast to allow efficient milling of the soft material, hence the larger particle size compared to low feed rate.

It is also worth noting that the 'pusher' nozzle did not appear to influence particle size as significantly as the 'grinding' nozzle (p>0.05). This phenomenon was also seen in the study performed by Vatsaraj *et al.* (11). Both grinding nozzle '1' and '2' pressures appeared to have different actions and reduced particle size more efficiently when they were inversely proportional to each other (i.e., grinding '1' at 100 psi and grinding '2' at 60 psi) at high 'pusher' pressures (100 psi).

Regarding the yield produced after milling, there was a loss of approximately 20%. The sample in this investigation was collected from the collecting vessel of the air-jet mill, which accounted for 80% yield as indicated. The remaining loss was associated with the interior surfaces of the air-jet mill, which highlights how the soft material properties may predispose the sample to adhesive or agglomerative losses within an air-jet mill. Some of the material may have deposited on air filters, but based on our mass balance calculations and material recovery, these amounts are likely to be small.

Thus, data achieved from this experiment provides evidence that, in order to achieve the smallest particle size, for a soft material using a lab-scale air-jet mill a low feed rate, high grinding '1', low grinding '2', and a high pusher pressure was required.

Combination of Micronization and Next Generation Impactor

In order to achieve particle size for aerosol delivery, the Pluronic® F-68 was milled directly into a cascade impactor, as the purpose of the study was to produce particles with diameters less than 5 μm. Optimized milling parameters achieved from air-jet milling investigations of low feed rate (0.14 g/min), grinding '1' (100 psi), grinding '2' (60 psi), pusher pressure (100 psi) where incorporated. Using the air-jet fluid energy mill alone only achieved a median particle size of approximately 24 μm, under optimum operating conditions according to the factorial design. Hence it was expected that as the NGI is used as a classification tool, pre-classified and acceptable materials for inhalation could be collected from the relevant NGI stage that correspond to diameters less than 5 μm and the yield calculated.

Consequently, when formulating a delivery system requiring the use of soft micronized materials, the combination of milling and NGI may be used to achieve this. However, this combination resulted in a low yield (1.9%) and thus may not be practical and cost-effective.

Cryo-Micro-Ball Mill

The results (Table 3) demonstrate that using cryo-micro-ball milling to reduce particle size of a soft material was a more efficient and effective process compared with air-jet milling. The particle size achieved was less than 10 μm after 15 min regardless of the starting weight of sample (Table 3). The process of micro-ball milling generated heat at ambient room temperature, resulting in degradation of Pluronic® F-68

Table III. Effect of Pluronic® F-68 Mass and Time on Particle Size Reduction (Dv50) (n=3)

	Time (mins)		
Mass (mg)	5	10	15
25	16.37±2.34 μm	12.69±3.90 μm	9.37±3.17 μm
50	15.54±3.26 μm	12.92±4.14 μm	8.47±0.28 μm
100	15.90±2.72 μm	12.75±1.01 μm	8.08±1.44 μm

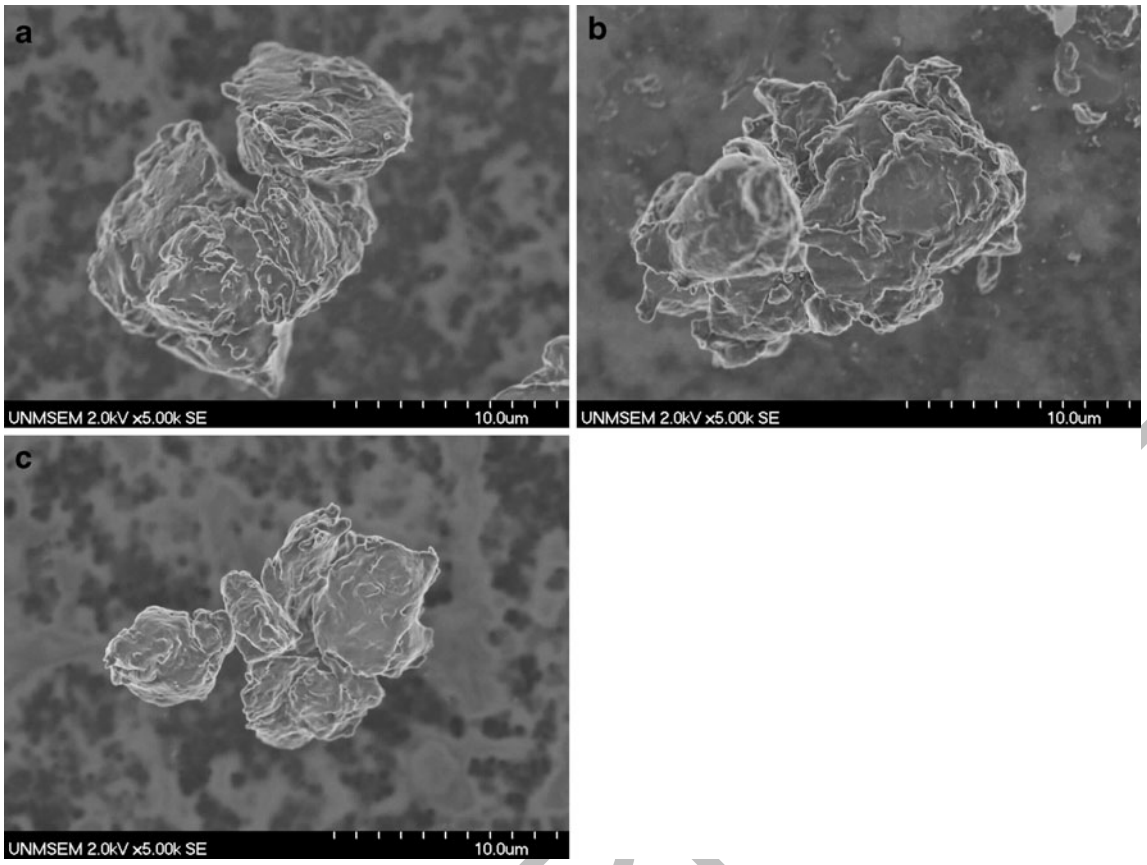

Fig. 4. SEM micrographs of cryo-micro-ball milled Pluronic® F-68 after 15 min for 25 mg (**a**), 50 mg (**b**), and 100 mg (**c**)

due to its low melting point (52°C). As a result, cryo-milling was used to avoid the solid temperature exceeding the glass transition temperature during the milling process by placing the micro-ball mill just above the surface of liquid nitrogen. A number of investigations have incorporated this method into their milling process. For example, Chieng *et al.* investigated the formation and stability of ranitidine hydrochloride amorphous state using cryo-milling performed with an oscillatory ball mill (26). Similarly, Garmise *et al.* investigated dry powder vaccine formulations using chitosan as a mucoadhesive compound suitable for nasal delivery (25). The chitosan, a soft material, was reduced to sizes suitable for nasal delivery using a cryo-milling technique because chitosan was not brittle at room temperature. Hence, their susceptibility to size reduction by a simple milling technique was compromised due to insufficient energy generated in overcoming the elastic properties, as shown in this study. However, no melting of Pluronic® F-68 was observed in the grinding chamber of the air-jet fluid energy mill.

Consequently, the use of liquid nitrogen served a dual purpose. Besides keeping the temperature low, the liquid nitrogen also increased the hardness of Pluronic® F-68, making it more brittle and decreasing the elastic properties. Thus, less energy was required to overcome the elastic limit of the material resulting in deformation and fracture, and eventually greater particle size reduction. Furthermore, liquid nitrogen changed the physical properties of the material, and as a result this needs to be investigated further to determine the cooling effect on particle size reduction using an air-jet fluid energy mill.

The results in Table 3 indicate that particle size reduction increased with milling time regardless of sample weight. This was the result of the input energy from the micro-ball mill, due to the frequency of revolutions, being directly proportional to the milling time. In this study, only one speed setting (FAST) was implemented, and thus it was most likely that the breakage in particles to a smaller size occurred predominantly during the impaction of the stainless steel ball bearing with the particles**,** leading to fracture, crushing, and attrition (21). For example, the particles interacted with each other, as well as the ball bearing and the sides of the chamber, resulting in particle breakage and the production of smaller particles, when the ball bearing was in the impact mode (31). This has been shown to occur when the stresses generated on the particles exceed the elastic limit causing permanent deformation and/or fracture leading to particle breakage (31). The stresses occur from the resulting compression, shear and impaction with particles and surface-particle interactions. Thus, results from the cryo-micro-ball milling experiments demonstrated a significant particle size reduction compared to the experiments performed using the air-jet mill and appeared to be a more efficient process at reducing particle size.

CONCLUSION

The results from this investigation represent that micronization of a soft material using a lab-scale air-jet mill may not be possible to achieve particle size of approximately 5 μm for pulmonary delivery. This was mostly due to the inefficiency of

the air-jet mill to overcome the elastic properties of the soft material. However, incorporating a freezing component to the milling process has the advantage of reducing the hardness and elastic properties of the material and hence, reducing the energy required by the mill to cause fracture and eventually particle break-up. Consequently, cryo-micro-ball milling may be a more efficient means of reducing particle size. Future investigations will involve optimizing the cryo-micro-ball mill process using other soft materials. In addition the possibility of incorporating a freezing component to the air-jet milling process will be evaluated.

ACKNOWLEDGMENTS

The authors would like to acknowledge that a portion of this work was performed by them when working at the College of Pharmacy, University of New Mexico, USA. The authors would also like to thank Dr Marwan Al-Haik at Department of Mechanical Engineering, School of Engineering, University of New Mexico, USA, for his help in using the nanotester 600 and determining the results.

REFERENCES

1. Posti J, Katila K, Kostianen T. Dissolution rate limited biovailability of flutamide, and *in vitro–in vivo* correlation. Eur J Pharm Biopharm. 2000;49(1):35–9.
2. Waterman CK, Sutton CS. A computational model for particle size influence on drug absorption during controlled-release colonic delivery. J Control Release. 2003;86(2–3):293–304.
3. Zeng XM, Martin GP, Tee SK, Abu A. Effects of particle size and adding sequence of fine lactose on the deposition of salbutamol sulphate from a dry powder formulation. Int J Pharm. 1999;133–44.
4. Steckel H, Müller B. *In vitro* evaluation of dry powder inhalers II: influence of carrier particle size and concentration on *in vitro* deposition. Int J Pharm. 1997;154(1):31–7.
5. Shoyele AS, Slowey A. Prospects of formulating proteins/peptides as aerosols for pulmonary drug delivery. Int J Pharm. 2006;314(1):1–8.
6. Gilani K, Najafabadi AR, Barghi M, Rafiee-Tehrani M. Aerosolisation of beclomethasone dipropionate using spray dried lactose/polyethylene glycol carriers. Eur J Pharm Biopharm. 2004;58(3):595–606.
7. Finlay WH, Stapleton KW, Zuberbuhler P. Fine particle fraction as measure of mass depositing in the lung inhalation of nearly isotonic nebulized aerosols. J Aerosol Sci. 1997;28(7).
8. Hickey A, Martonen BT, Yang Y. Theoretical relationship of lung deposition to the fine particle fraction of inhalation aerosols. Pharm Acta Helv. 1996;71(3):185–90.
9. Newman PS, Wilding RI, Hirst HP. Human lung deposition data: the bridge between *in vitro* and clinical evaluations for inhaled drug products. Int J Pharm. 2000;208(1–2):49–60.
10. Irngartinger M, Camuglia V, Damm M, Goede J, Frijlink HW. Pulmonary delivery of therapeutic peptides via dry powder inhalation: effects of micronisation and manufacturing. Eur J Pharm Biopharm. 2004;58(1):7–14.
11. Vatsaraj BN, Gao D, Kowalski LD. Optimization of the operating conditions of a lab scale aljet mill using lactose and sucrose: a technical note. AAPS PharmSciTech. 2003;4(2):p. Article 27.
12. Tanaka T, Kanda Y. Crushing and grinding. In: Masuda H, Higashitani K, Yoshida H, editors. Powder technology handbook. 3rd ed. New York: CRC Taylor and Francis; 2006.
13. Gilvarry JJ. Fracture of brittle solids, I. J Appl Phys. 1961;32:391–9.
14. Gaudin AM, Meloy TP. Trans AIME. 1962;223:43–51.
15. Broadbent SR, Calcott TG. Coal breakage processes:l a new analysis of coal breakage processes. J Inst Fuel. 1956;29:524–8.
16. Chujo K. Kagaku Kougaku Kagakukikai. 1949;7:1–83.
17. Taylor LJ, Papadopoulos DG, Dunn PJ, Bentham AC, Mitchell JC, Snowden MJ. Mechanical characterisation of powders using nanoindentation. Powder Technol. 2004;143–144:179–85.
18. Hancock BC, Clas SD, Christensen K. Micro-scale measurement of the mechanical properties of compressed pharmaceutical powders. 1: the elasticity and fracture behaviour of microcrystalline cellulose. Int J Pharm. 2000;209(1–2):27–35.
19. York P, Bassam F, Rowe RC, Roberts RJ. Fracture mechanics of microcrystalline cellulose powders. Int J Pharm. 1990;66:143–8.
20. Batrakova EV, Li S, Li Y, Alakhov VY, Kabanov AV. Effect of pluronic P85 on ATPase activity of drug efflux transporters. Pharm Res. 2004;12:2226–33.
21. Batrakova EV, Kabanov AV. Pluronic block copolymers: evolution of drug delivery concept from inert nanocarriers to biological response modifiers. J Control Release. 2008;130(2):98–106.
22. Xiong XY, Tam KC, Gan LH. Polymeric nanostructures for drug delivery applications based on Pluronic copolymer systems. J Nanosci Nanotechnol. 2006;6(9–10):2638–50.
23. El-Sherbiny IM, McGill S, Smyth HD. Swellable microparticles as carriers for sustained pulmonary drug delivery. J Pharm Sci. 2010;99(5):2343–56.
24. Yang YT, Chen CT, Yang JC, Tsai T. Spray-dried microparticles containing polymeric micelles encapsulating hematroporphyrin. AAPS J. 2010;12(2):138–46.
25. Garmise RJ, Mar K, Crowder TM, Hwang CR, Ferriter M, Huang J, *et al*. Formulation of a dry powder influenza vaccine for nasal delivery. AAPS PharmSciTech. 2006;10(7):E19.
26. Chieng N, Rades T, Saville D. Formation and physical stability of the amorphous phase of ranitidine hydrochloride polymorphs prepared by cryo-milling. Eur J Pharm Biopharm. 2008;68(3):771–80.
27. Shaik MS, Haynes A, McSween J, Ikediobi O, Kanikkannan N, Singh M. Inhalation delivery of anticancer agents via HFA-based metered dose inhaler using methotrexate as a model drug. J Aerosol Med. 2002;15(3):261–70.
28. Duncan-Hewitt WC, Weatherley GC. Evaluating the hardness, Young's modulus, and fracture toughness of some pharmaceutical crystals using microindentation techniques. J Mater Sci Lett. 1989;8(11):1350–2.
29. Zugner S, Marquardt K, Zimmermann I. Influence of nanomechanical crystal properties on the comminution process of particulate solids in spiral jet mills. Eur J Pharm Biopharm. 2006;62:194–201.
30. Liao X, Wiedmann TS. Characterization of pharmaceutical solids by scanning probe microscopy. J Pharm Sci. 2004;93(9):2250–8.
31. Chen Y, Ding Y, Papadopoulos DG, Ghadiri M. Energy-based analysis of milling α-lactose monohydrate. J Pharm Sci. 2004;93(4):886–95.